

The Stabilization of Asphaltenes in Different Crude Fractions: A Molecular Approach

Faissen B. Lordeiro,^{a,b} Rodrigo Altoé,^c Daniela Hartmann,^b Eduardo J. M. Filipe,^a
Gaspar González*^c and Elizabete F. Lucas^{b,c}

^aCentro de Química Estrutural, Instituto Superior Técnico, Universidade de Lisboa,
1049-001 Lisboa, Portugal

^bLaboratório de Aditivos Poliméricos para Produção de Petróleo, COPPE/PEMM,
Universidade Federal do Rio de Janeiro, 21941-598 Rio de Janeiro-RJ, Brazil

^cLaboratório de Macromoléculas e Coloides na Indústria do Petróleo, Instituto de Macromoléculas,
Universidade Federal do Rio de Janeiro, 21941-594 Rio de Janeiro-RJ, Brazil

The conditions of petroleum extraction may allow asphaltenes to precipitate, causing deposition that clogs wells, pipes and equipment, consequently reducing productivity. In this work, the solubility parameters and precipitation onset of polar fractions of heavy crudes from Brazilian fields were estimated using a simplified system of *n*-heptane/toluene mixtures. Asphaltenes were extracted by two different methods with regard to pressure and temperature. The samples were physically and chemically characterized, and both density (1053-1159 kg m⁻³) and molecular weight (1176-5316 g mol⁻¹) were estimated based on the density of diluted asphaltenes in toluene solutions. The solubility of those fractions was studied as well as their solubility parameter (ca. 19-23 MPa^{0.5}) based on regular solution theory, Flory-Huggins theory and empirical correlation. The influence of asphaltene concentration (between 0.5 and 5.0 g L⁻¹) on the solubility parameter and precipitation onset was studied, and a strong linear correlation between them was not found.

Keywords: asphaltenes, solid residue, solubility parameter, precipitation onset, *n*-heptane/toluene mixtures

Introduction

Crude oil is a complex mixture of hydrocarbons with small quantities of nitrogen (N), oxygen (O) and sulfur (S), as well as traces of metals such as vanadium (V) and nickel (Ni).¹ Generally the percentage of oxygen is lower than that of sulfur. The former element is responsible for the acidity of oil and is found in the form of phenols, carboxylic acids, furans and esters, while the latter can be in elemental form or in the form of sulfides, such as H₂S, among others. The nitrogen compounds are usually found in the heaviest fractions, resins and asphaltenes, whose boiling point is higher than 250 °C, in the form of pyridines, amides and amines.² Mainly due to the depletion of many light crude reserves, the global trend is for greater reliance on heavy crudes, with lower quality, as forecast by the Organization of the Petroleum Exporting Countries (OPEC). The high

viscosity of heavy crude hampers its flow and causes other serious problems during extraction, transport and refining.^{3,4} A high content of asphaltenes ($\geq 6\%$ m m⁻¹) generally causes delayed ignition and incomplete fuel combustion, resulting in greater emission of particulate matter in the atmosphere, among other problems.⁵ In many cases, asphaltenes are the main constituent of organic matter in blockages.⁶ The agglomeration and formation of scales caused by the deposition of asphaltenes also reduces the production rate.⁷ Problems related to asphaltenes deposition can also occur during CO₂ flooding.⁸ Furthermore, the stability of water-in-crude oil emulsions and wax precipitation are also somewhat associated with the asphaltene fractions.⁹⁻¹⁴

The asphaltenes contained in petroleum are defined as the fractions soluble in aromatic solvents, such as toluene, but insoluble in alkanes, such as *n*-heptane.¹⁵⁻¹⁷ They are generally obtained by precipitation in apolar solvents like *n*-pentane and *n*-heptane (among others), at atmospheric or high pressure.¹⁸ They are also soluble in liquids with

*e-mail: zoilogaspar@yahoo.co.uk

high surface tension, such as pyridine, carbon tetrachloride (CCl_4) and carbon disulfide (CS_2).¹⁵ Asphaltenes are composed mainly of carbon and hydrogen, but they can also contain small quantities of nitrogen (0.6 to 3.3%), oxygen (0.3 to 4.9%),⁵ and sulfur (0.3 to 10.3%),⁵ along with traces of heavy metals like vanadium and nickel.¹⁵ Boduszinski *et al.*¹⁹ reported that the concentration of heteroatoms varies monotonically with polarity, so that all the fractions of crude oil contain these elements, although they are more concentrated in the more polar fractions. These compounds have complex structures.¹⁵ Basically, asphaltenes can be described as polyaromatic hydrocarbons with different functional groups dispersed in apparently random form.^{20,21} The literature²² contains estimates of the molar mass of asphaltenes ranging from 1,000 to 30,000 g mol^{-1} . This wide variation can be explained by the formation of molecular aggregates, where a larger number of molecules in the aggregate is associated with a higher molar mass value, as indicated by laboratory experiments.²³ In this respect, it has been reported²² that the higher the concentration of asphaltenes, the greater will be the molar mass value found experimentally. The most accepted molar mass range for an asphaltene molecule is from about 750^{24,25} to 2,000 g mol^{-1} .¹⁹ It must be also take in account that the molar mass depends on the solvent used to isolated the asphaltene molecules from the crude oil.²⁶

At refineries, the fraction with highest asphaltene percentage is called asphalt. It is obtained by the deasphaltation process, where the load-vacuum residue (VR) from a vacuum distillation column-is separated into two fractions. Deasphalting is widely used through a liquid-liquid extraction process that uses light paraffinic solvents such as *n*-pentane.^{27,28} Many recent experimental and theoretical studies and reviews have been published²⁹⁻³⁴ due to the relevance of asphaltenes associated with their complexity.

The solubility parameter (δ , $\text{MPa}^{0.5}$) indicates the ability of a given solvent or mixture of solvents to dissolve a solute. This parameter can be obtained by applying equation 1,³⁵ where c is the cohesive energy density (CED, MPa), ΔH_{vap} is the vaporization enthalpy ($\text{MPa m}^3 \text{mol}^{-1}$), R is the universal gas constant ($8.31 \times 10^{-6} \text{MPa m}^3 \text{mol}^{-1} \text{K}^{-1}$), T is the temperature (K) and v is the molar volume ($\text{m}^3 \text{mol}^{-1}$). Just as the solubility of two materials occurs when there is similarity between the attractive forces of the solute and solvent, these materials are expected to be miscible if the two cohesive energy densities have the same order of magnitude.

$$\delta_s = \sqrt{c} = \sqrt{\frac{\Delta H_{\text{vap}} - RT}{v}} \quad (1)$$

An important tool for prediction properties of materials like bitumen, crude oil, maltenes and asphaltenes is solubility parameters or other cohesion parameters.³⁶⁻³⁸ A wide review about solubility parameters and their versatility to deal with solubility and other properties of petroleum and fossil liquids and solids, was presented by researchers in theoretical and experimental points of view. The use of reliable methods as HSP (Hansen solubility parameter) leads to predict thermodynamic interactions and solubility with solids and liquids that have their solubility parameters published. Such results are in agreement with aggregation/dispersion of asphaltenes, asphaltene colloidal behavior and structure, solubility properties, adsorption, flocculation, vaporization, and molecular weight discussions.³⁷ The HSP of asphaltenes obtained from oil sand bitumen samples and a vacuum residue fraction can be determined by the method of Hansen solubility sphere.³⁸ Although the Hansen solubility parameter usually supplies a better approximation, by considering hydrogen bonding and polar interactions, the prediction of Hildebrand solubility parameters has been extensively used.³⁹

The solubility parameter is very useful to predict the phase behavior of different types of systems, including liquid-solid ones,^{36,40} and it has been experimentally determined, for low molar mass compounds, by different techniques.⁴¹ Among the methods to estimate the solubility parameter are application of the Scatchard-Hildebrand (SH) equation or Flory-Huggins (FH) model and empirical correlation. The theory of regular solutions can be used to describe the properties of mixtures simply. It involves a simple model, but is more complex than the ideal solution model, since it considers the interaction of the different components in a solution. In this model, it is assumed that the mixture does not generate a change in volume and that the mixture's entropy is equal to the entropy of an ideal solution, with the excess entropy (S^E) being zero. The main problem of applying the theory of regular solutions to asphaltenes is that it does not take into account the sample polydispersivity and the fact that asphaltenes form aggregates, a limitation that could be overcome by calculating the solubility parameters for dimers and trimers. Nevertheless, it is very useful, since the solubility parameter can be estimated based on experimental data.⁴² Equation 2, suggested by Scatchard and Hildebrand, is based on the theory of regular solutions and the fact that molecules are linked by van der Waals forces.³⁵ When the physical state of molecules is altered by an input of energy, it is possible to quantify the energy necessary to break the intermolecular interactions. Hence, the relation between vaporization and van der Waals forces can be translated to a relation between vaporization and solubility.⁴³

$$RT \ln(\gamma_i) = RT \ln\left(\frac{a_i}{x_i}\right) = \frac{MW_i}{\rho_i} \phi_s^2 (\delta_i - \delta_s)^2 = v_i N_s^2 (\delta_i - \delta_s)^2 \quad (2)$$

where R is the universal gas constant (8.31×10^{-6} MPa m³ mol⁻¹ K⁻¹); T is the temperature (K); γ_i , a_i , x_i , MW_i , ρ_i , δ_i and v_i are the coefficient of activity, activity, molar fraction, molar weight (kg mol⁻¹), density (kg m⁻³), solubility parameter (MPa^{0.5}) and molar volume (m³ mol⁻¹) of solute i , respectively; and N_s and δ_s are the volumetric fraction and solubility parameter (MPa^{0.5}) of solvent s , respectively. Since the volume of asphaltenes in comparison with the volume of the solvent is negligible, it is assumed that $\phi_s = 1$. Besides this, in the case of pure asphaltenes in equilibrium, such as asphaltenes in a saturated solution, the latter's activity is unitary ($a_i = 1$).^{42,43} Rearranging the equations yields equation 3, which can be used to estimate the solubility parameter of the polar fractions of crude oil.

$$\delta_i = \delta_s + \sqrt{-\frac{RT \ln(x_i) \rho_i}{MW_i}} \quad (3)$$

Considering the variation of entropy due to the mixture and combining the Scatchard-Hildebrand equation with the Flory-Huggins theory leads to equation 4.⁴⁴

$$\ln(\phi_i) = \frac{v_i}{v_s} - 1 - \frac{v_i}{RT} (\delta_i - \delta_s)^2 \quad (4)$$

where ϕ_i is the volumetric fraction of solute i and v_i and v_s are the molar volume of solute i and solvent s , respectively. Therefore, equation 4 can be reorganized into equation 5.

$$\delta_i = \delta_s + \sqrt{\frac{\ln(\phi_i) + 1 - \frac{v_i}{v_s}}{-\frac{v_i}{RT}}} \quad (5)$$

The literature contains many studies describing attempts to estimate the solubility parameters of asphaltenes based on experimental data. The following correlation is based on the idea that asphaltenes are polyaromatic hydrocarbons with aggregated functional groups that are randomly distributed, can be treated as a homologous series, which solubility parameter and molar volume distributions are calculated from experimental measurements of density and molar mass. Asphaltene solubility parameter, molar volume and density are correlated with molar mass.²⁰ In light of these characteristics, one can assume that the vaporization enthalpy varies linearly with the molar mass, leading to equation 6.

$$\delta_i = \sqrt{\frac{\Delta H_{\text{vap},i} - RT}{v_i}} = \sqrt{\frac{KMW_i + Z - RT}{\frac{MW_i}{\rho_i}}} \quad (6)$$

where $\Delta H_{\text{vap},i}$, v_i , MW_i and ρ_i are the vaporization enthalpy, molar volume, molar weight and density of solute i , respectively; K and Z are parameters of linear dependence of the vaporization enthalpy with the molar mass; R is the universal gas constant; and T is the temperature. For compounds like asphaltenes, with high molar mass, the term $Z - RT$ has negligible values in comparison with the term KMW_i (-3 kJ mol⁻¹ compared with a minimum value of 400 kJ mol⁻¹), so in these cases equation 6 can be modified to equation 7.²⁰

$$\delta_i = \sqrt{K\rho_i} \quad (7)$$

According to the proponents of this correlation method, the constant K should have values between alkanes and naphthalenes, 270 and 398 J g⁻¹, respectively, and it is necessary to determine them indirectly using experimental solubility data. Given that asphaltene aromaticity increases with increasing molar mass, as expected, in their study, the value of K of 367 J g⁻¹ best fit the experimental data and the value was nearer that of the naphthalenes.²⁰

Kinetics and thermodynamics aspects must be considered when studying asphaltenes sedimentation/deposition. Fogler and co-workers^{45,46} have dedicated special attention to this theme. They have demonstrated that the time required to precipitate asphaltenes can vary from a few minutes to several months, and established that the solubility of asphaltenes is function of the precipitant concentration. Moreover, they have demonstrated how air and nitrogen affect the kinetics of asphaltenes precipitation.^{45,46}

Several procedures have been used to measure the asphaltenes precipitation onset induced by n -alkanes, and all of them present advantages and disadvantages. Gravimetric method, optical microscopy technique, and viscosity, refractive index and density measurements are some examples. Presumably, ultraviolet-visible (UV-Vis) and near-infrared (NIR) spectroscopy techniques are the most common analytical methods applied to study asphaltenes stabilization. However, the crude oil dilution is not required when using NIR, being more representative of real systems.^{47,48}

The aim of the present study is to analyze the most polar fraction of crude oil, asphaltenes, to predict the conditions under which they will precipitate in industrial settings (e.g., storage tanks or processing/refining equipment), and during extraction. This is relevant since the deposition of asphaltenes

reduces the flow both of crude oil and refined products, requiring shut-downs for cleaning and thus higher costs.

Experimental

Materials

Two crude oil samples from Brazilian fields, called PET A and PET B, were donated by Petrobras, Rio de Janeiro, Brazil. An asphaltic residue, called ASPR C, was obtained from the Duque de Caxias refinery, whose deasphalting unit operates with propane. Toluene, *n*-heptane and chloroform, with purity > 99%, were purchased from Vetec Química Fina Ltda., Duque de Caxias, Brazil. Methanol, with purity > 99%, was acquired from Petroquímicos Ltda. (Ribeirão Preto, Brazil). Propane, with purity > 99%, was purchased from Air Liquid São Paulo, Brazil (kept at room temperature in 45 kg cylinders), and KBr was purchased from Celtic Chemicals, Port Talbot, United Kingdom. All the chemical reagents were used without additional purification.

Extraction of asphaltene C7I from the crude oil samples and the asphaltic residue

We used two methods to extract the asphaltene C7I from the crude oil. In the first, designated method 1, the asphaltenes were extracted according to the standard IP 143⁴⁹ and a protocol described previously.⁵⁰ Method 2 involved the separation of the crude oil into a solid fraction (henceforth called solid residue or SR) and a liquid fraction (liquid extract, or LE), employing propane. This separation was performed at high pressure and temperature (40 bar and 70 °C). This solid residue was composed of asphaltenes and maltenes, which in turn were separated similarly to method 1. It is important to mention that in the case of the asphaltic residue under study (ASPR C), the fraction of asphaltenes was obtained only by method 1.

Method 1

The procedure to extract asphaltene C7I from the crude oil and asphaltic residue consisted of four steps, illustrated in Figure 1: precipitation (*n*-heptane), filtration, extraction-purification (*n*-heptane followed by toluene) and drying.⁵¹ Since asphaltenes are sensitive to light and air,⁴⁶ with the possible occurrence of oxidation, the samples were kept sealed in the dark by covering the storage flasks with aluminum foil.

Method 2

Figure 2 contains a diagram of the system used. In

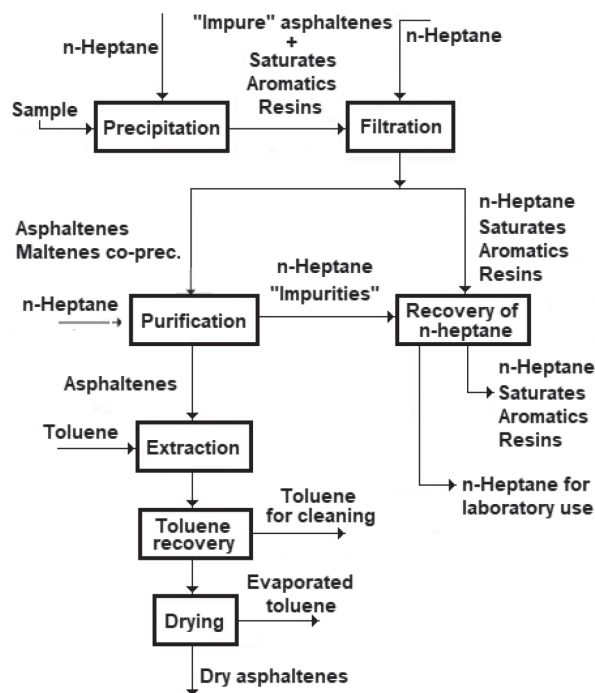


Figure 1. Diagram of the steps for extraction of asphaltenes by method 1.

this case, the crude oil was separated into a solid residue and liquid extract based on the solubility of these two in propane, at high pressure and temperature. From the solid residue so obtained, it was possible also to separate the asphaltene C7I.⁵²

Extraction of solid residue from the crude oil: first we placed a determined mass (100 g) of crude oil at 70 °C in cylinder B (Figure 2), created a vacuum and then pressurized the system by introducing water in the base of cylinder B with a pneumatic pump (Heskel) to attain a pressure of 40 bar. Then, we introduced 1 L of liquid propane from cylinder A into cylinder B, draining part of the water contained under the piston (cylinder B). After attaining an oil/propane ratio of 1/10, we adjusted the pressure to 40 bar and the temperature to 70 °C and isolated the cylinder containing the mixture (cylinder B) by closing the valves. We then activated the agitation system for 5 h, followed by leaving the system at rest for 18 h to allow separation into two phases (liquid extract and solid residue). Next, we opened valve V1 and directed the liquid extract into a collector, followed by removal of the residual propane with a vacuum pump for 2 h at 60 °C (under these conditions, the propane evaporated from the system). Finally, we recovered the solid phase (solid residue) from cylinder B and saved it for subsequent treatment.

Extraction of asphaltenes C7I from the solid residue: after extraction of the solid residue from the oil sample, we separated the asphaltenes from the maltenes. For this purpose, we weighed a determined mass in a beaker and added *n*-heptane

at a ratio of 30 mL of solvent *per* gram of solid residue, and then wrapped the beaker in plastic film and aluminum foil to prevent vaporization of the solvent and oxidation of the asphaltenes, and placed it under stirring for 24 h at room temperature. Finally, we filtered and dried the sample.

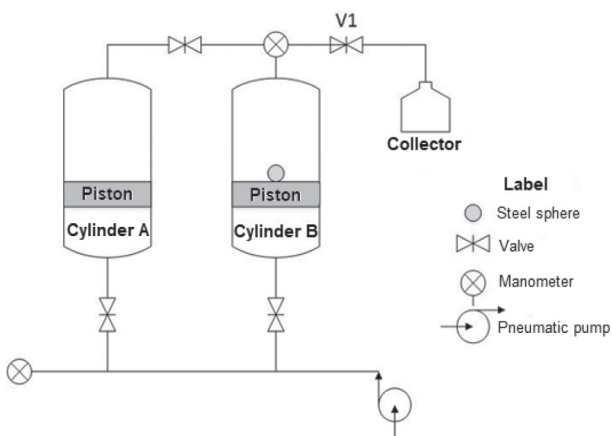


Figure 2. Diagram of the equipment used for extraction of the solid residue by method 2.

Characterization of the crude oil samples and respective fractions

The crude oil and/or respective fractions were characterized regarding water content, density, °API (degree of American Petroleum Institute), elemental composition (CHNS-O) and SARA composition (saturates, aromatics, resins and asphaltenes). Fourier-transform infrared (FTIR) spectra were also obtained.

The water content of each crude oil sample was determined with a Karl-Fischer titrator (Metrohm, 870 KF Titrino plus). The density and °API of the crude oils were determined with a density meter (Anton Paar, DMA 4500 M). The concentrations of CHNS-O were measured with a CHNS-O elemental analyzer (Thermo Finnigan, EA1). The contents of C, H, S and N were quantified by combustion followed by chromatography, while the content of oxygen was determined by difference (subject to greater error). The limit of detection of the device is 0.3%, so when the content of any of the elements was below this threshold, we assumed the value was 0.3% to enable estimating the oxygen content. The H/C molar ratio was calculated based on the molar masses of the elements and the respective percentages. The contents of saturates, aromatics, resins and asphaltenes (SARA) were determined through a modified TLC-FID device (thin-layer chromatograph with flame ionization detector). In this step, the asphaltenes were separated and quantified by the IP-143 procedure.⁴⁹ The sample of asphaltenes was also separated by microdistillation into two fractions according to the

boiling temperature (T_B), $T_B < 260^\circ\text{C}$ and $T_B > 260^\circ\text{C}$. The first was separated into two other fractions, saturates (S1) and aromatics (A1), via supercritical fluid chromatography (SFC) with CS_2 . The fraction with boiling point $> 260^\circ\text{C}$ was fractionated by TLC-FID into heavy saturates (S2), heavy aromatics (A2) and polar fraction (P1). Thus, the saturates corresponded to fractions S1 + S2, the aromatics corresponded to fractions A1 + A2 and the resins to fraction P1 (containing the asphaltenes).

The FTIR spectra were obtained with an FTIR/FIR spectrophotometer (PerkinElmer, Frontier) in the region between 400 and 4000 cm^{-1} , in transmission mode, with resolution of 4 cm^{-1} . The solid samples were prepared in KBr pellets while the liquid samples were studied in the form of thin films. The spectra were acquired with an average of 20 scans.

Determination of the precipitation onset of the asphaltenes by titration with *n*-heptane

The assay consisted of determining the volume of *n*-heptane necessary to start precipitation of the asphaltenes in different samples during the titration of this non-solvent. This assay was performed in samples of crude oil and of two distinct model systems (asphaltene C7I in toluene and solid residue in toluene) and was based on a protocol described previously.^{50,52-54} Near-infrared (NIR) spectroscopy was applied to detect the variations in the systems, with absorbance readings at 1600 nm, using a Bruker Matrix-F NIR spectrophotometer with a probe having an optical path of 5 mm and a Varian ProStar 210 positive displacement pump, at an *n*-heptane flow of 2 mL min^{-1} . The device was configured to enable absorbance readings for 20 min at 30-s intervals, so that each measurement corresponded to the addition of 1 mL of *n*-heptane. The volume of *n*-heptane was considered to be that value at lowest absorbance, and the precipitation onset was expressed in terms of volume of *n*-heptane (mL) *per* gram of crude oil or model system. The model solutions were prepared with about 0.125 g of asphaltenes in 25 mL of toluene (0.5% m v^{-1}), homogenized in a Bandelin Sonorex ultrasound bath for 10 min at room temperature. The solid residue solutions in toluene were prepared at a concentration of 15 g L^{-1} , due to the low absorbance values presented by these residues at 1600 nm. The tests were performed in duplicate.

Determination of the precipitation onset with constant concentration of asphaltenes

The precipitation of asphaltenes was also evaluated in systems containing solvents with different solubility

parameters and constant concentration of asphaltenes. Based on the quality of the solvent, the precipitation of asphaltenes can be induced and detected by the reduction of the concentration of asphaltenes in solution, employing ultraviolet spectrometry. For this purpose, we used a Varian Cary 50 UV-Vis spectrophotometer, with readings at a wavelength of 850 nm. In this case, only the model systems (asphaltenes in toluene and solid residue in toluene) were evaluated, since this technique is not able to analyze petroleum samples. The test, although not identifying the precipitation onset with the same precision as the method employing titration of *n*-heptane, allows determining the quantity of asphaltenes precipitated. For that purpose, it is necessary to obtain a response curve of absorption intensity in function of concentration of asphaltenes or solid residue in toluene.

Obtaining the response curve

A stock solution of asphaltic material in toluene was prepared by dissolving 0.5 g of solid asphaltic material in 100 mL of toluene, to obtain a final concentration of 5 g L⁻¹. Then, each of 10 centrifuge tubes was filled with 1.0 mL of this stock solution and the volume was completed to 10 mL with mixtures of the solvents toluene/*n*-heptane in varied proportions. The initial concentration of asphaltenes in each mixture was around 500 ppm. Each solution was homogenized for 5 min in an ultrasound bath at room temperature and then left at rest for 2 h. Next, each tube was centrifuged for 10 min and 2000 rpm in a Boeco Ipas centrifuge. Finally, the absorbance of the supernatant was read at the respective characteristic wavelength. With the resulting data it was possible to determine the final concentration of each supernatant and plot a graph

of final concentration *versus* percentage of *n*-heptane in the mixture. In the case of the solid residues, besides asphaltenes, these also contained maltenes, which are soluble in *n*-heptane. We prepared a solution of 0.5 g L⁻¹ of solid residues in *n*-heptane (0.01 g of solid residues in 20 mL of *n*-heptane) and read the absorbance to verify the solubility value of the solid residues in *n*-heptane and predict the minimum absorbance value in the solid residue precipitation test.

Results and Discussion

Characterization of the crude oil samples and their fractions

The crude oil samples and the respective liquid extracts (LE) were characterized regarding density, °API, elemental analyses and SARA content. The oil samples were also characterized regarding water content. The SARA analysis was carried out for the solid residues A and B, denoted by SR A and SR B. The elemental analysis was performed for these samples and the asphaltene fractions obtained. The results are reported in Tables 1 and 2.

The crude oil samples were classified as heavy oils (°API < 22.3).⁵⁵ Crude oil B (PET B) was found to be slightly heavier than crude oil A (PET A), due to its higher density. On the contrary, liquid extract A (LE A) was heavier than liquid extract B (LE B). Since liquid extract B was lighter, we expected crude oil B also to be lighter than crude oil A. However, this was not the case, since PET B had a greater relative quantity of solid residue (41%) than PET A (29%), although this difference could also have been due to the greater quantity of brine (denser than crude oil) in sample B.

Table 1. Results of the elemental analysis, water content, density and °API

Extraction method	Sample	H ₂ O / %	$\rho^{20^\circ\text{C}} / (\text{g cm}^{-3})$	°API (60 °F)	C / %	H / %	N / %	S / %	O / %	H/C
–	PET A	0.6	0.9724	13.4	86.4	11.4	0.6	0.3 ^a	1.3	1.57
–	PET B	2.9	0.9747	13.1	85.8	11.7	0.7	0.7	1.1	1.62
1	ASPH A	–	–	–	85.8	7.7	0.9	0.3 ^l	5.3	1.07
	ASPH B	–	–	–	84.8	8.9	2.1	1.2	3.0	1.25
	ASPH C	–	–	–	83.0	8.8	1.6	2.8	3.8	1.26
2	SR A	–	–	–	87.7	9.5	0.3 ^a	0.5	2.0	1.29
	SR B	–	–	–	84.9	10.0	0.6	0.9	3.6	1.40
	LE A	–	0.9309	19.8	87.6	12.4	0.0 ^b	0.0 ^b	0.0	1.68
	LE B	–	0.9240	20.9	86.5	12.1	0.3 ^a	0.3 ^a	0.8	1.66

^aAssumed to be 0.3% since it was below the limit of detection of the device; ^bassumed to be 0.0 since the percentages of C and H together totaled 100%, although the value obtained in the analysis was < 0.3% (limit of detection of the device). PET: crude oil; ASPH: asphaltenes; SR: solid residue; LE: liquid extract; $\rho^{20^\circ\text{C}}$: density at 20 °C; °API: degree of American Petroleum Institute; C: carbon; H: hydrogen; N: nitrogen; S: sulfur; O: oxygen; H/C: hydrogen/carbon ratio.

Table 2. Results of the SARA analysis

Extraction method	Sample	Saturated / %	Aromatics / %	Resins / %	Asphaltenes / %
–	PET A	41.9	35.9	14.6	7.6
–	PET B	29.2	23.6	41.2	6.0
	SR A	1.4	30.1	20.9	47.6
	SR B	1.4	16.4	39.6	42.7
2	LE A	47.4	40.1	12.0	0.5
	LE B	47.1	35.2	17.2	0.6

SARA: saturated, aromatics, resins and asphaltenes; PET: crude oil; SR: solid residue; LE: liquid extract.

The greater the H/C ratio, the greater will be the saturation of the sample (more single C–H bonds than double or triple C–C bonds). Therefore, for both PET A and PET B, the saturation degree increased in the following order: asphaltenes < solid residue < crude oil < liquid extract. These results are in accordance with the fact that asphaltene molecules contain polyaromatic rings-where double bonds between carbons predominate. The liquid extract samples presented the highest H/C ratio values, which is coherent with their deasphaltation.

Furthermore, the liquid extracts A and B presented smaller heteroatom content than the respective residues, which was expected by the theory of compositional continuity of petroleum of Boduszynski *et al.*,¹⁹ according to which the concentration of heteroatoms varies monotonically with polarity.

The SARA analysis showed that both the solid residues (SR A and SR B) and the liquid extracts (LE A and LE B) were composed of all the fractions (saturates, aromatics, resins and asphaltenes) present in the respective crude oils, but with different percentages. The extraction method 2 separated the crude oil samples into a fraction rich in saturates and aromatics (liquid extract) and a fraction rich in resins and asphaltenes (solid residue). This distribution is in line with the theory of compositional continuity.¹⁹

Both the denser oil (PET B) and the denser liquid extract (LE A) contained a smaller concentration of asphaltenes than the respective less dense samples of oil (PET A) and liquid extract (LE B). This is not in line with that reported elsewhere in the literature,⁵⁶ according to which the density increases with the content of asphaltenes. As mentioned before, PET B is denser than PET A, since it contains a greater relative quantity of heavier fractions (resins and asphaltenes), although presenting a lower content of asphaltenes. Besides this, both the crude oil samples have an asphaltene percentage greater than or equal to 6%. In light oils, these values are significantly lower (some contain around 0.5% asphaltenes), meaning that the extraction of asphaltenes

from these oils requires the use of higher quantities of solvents, and consequently higher costs, which justifies the choice of the heavy oils in this study.

We obtained FTIR spectra for all the samples (see Supplementary Information (SI) section). As also observed by González *et al.*⁵⁷ the samples presented maximum absorbance values at very similar wavenumbers.

Determination of the precipitation onset of asphaltenes by titration with *n*-heptane and detection by near-infrared (NIR) spectroscopy

Figure 3 shows the curve of absorbance *versus* volume of *n*-heptane (mL) by mass of sample (g) for crude oil A (PET A).^{58,59} This curve does not contemplate point zero, since it was necessary first to add 1.0 mL of *n*-heptane *per g* of oil to increase the sample's fluidity. This procedure was carried out due to the high viscosity of the oil, which hampers its agitation, and thus its homogenization, while adding the solvent (*n*-heptane) during the test. As mentioned previously, the onset values are obtained at the minimum absorbances of each analysis, and the PET A presented a precipitation onset of asphaltenes of 3.5 mL of *n*-heptane *per g* of oil.

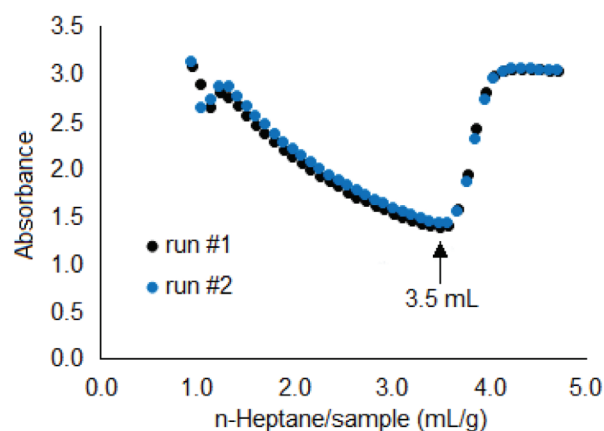


Figure 3. Asphaltenes precipitation onset determined by titration with *n*-heptane and detection with NIR spectroscopy for crude oil A (PET A).

Table 3 reports all precipitation onset values found. In general, the greater the volume of *n*-heptane necessary to precipitate the asphaltenes, the more stable the sample will be, and hence the lower will be the tendency to form scaling or clogging of equipment resulting from the deposition of asphaltenes.⁶⁰ Between PET A and PET B, the former was more stable than the latter with respect to asphaltene precipitation.

For a long time it was accepted that resins were responsible for the stabilization of asphaltenes.^{61,62} However, more recent experiments have shown that besides resins, aromatics also exert an influence on the maintenance of asphaltenes dissolved in crude oil.⁶³ The results obtained in this study show the strong influence of aromatics on the stabilization of asphaltenes in petroleum, since PET A, with a slightly higher concentration of asphaltenes than PET B, was more stable even though having a concentration of resins nearly 3 times lower. This can probably be attributed to the fact it has a 50% higher content of aromatics (Table 2). Besides this, according to the H/C ratio results (Table 1), the asphaltenes present in PET A were slightly more concentrated in saturated bonds than found in PET B, hampering their stabilization in the medium. Nevertheless, this sample was found to be more stable due to the relatively higher content of aromatics.

According to the analysis of the stability of the asphaltenes extracted from PET A, PET B and ASPH C by method 1, the system of asphaltenes A in toluene was more unstable than asphaltenes B and C. With respect to the elemental composition (Table 1) of these asphaltene fractions, ASPH A had a lower H/C ratio than samples ASPH B and ASPH C, thus having a higher unsaturation degree, which can contribute to its lower stability in relation to ASPH B and ASPH C. Besides this, although ASPH B and ASPH C contained higher levels of nitrogen and sulfur, ASPH A had a higher content of oxygen, a more electronegative element than N and S, thus contributing to its more polar character and thus lower stability. ASPH C

solution presented intermediate stability between ASPH A and ASPH B solutions. Since the H/C ratios of ASPH B and ASPH C were very similar, the greater stability of ASPH B in relation to ASPH C was likely related to its more polar character, since it has greater oxygen and sulfur contents than ASPH B.

Finally, for the asphaltene precipitation onset results of the solid residue systems obtained by method 2 (dissolved in toluene), a similar analysis to that undertaken for the asphaltene fraction solutions is possible: the explanation for the behavior of the solid residue solutions can be based on their elemental composition. SR B, although having a slightly higher H/C ratio than that of SR A, has higher levels of more polar elements (O, N and S) than SR A (Table 1), which is in accordance with the lower stability of SR B. Besides this, although SR B has twice the resin content of SR A, the latter has twice the content of aromatics, so SR A is more stable than SR B, in line with the previous observation regarding the stability by the aromatics.

Although the units of the asphaltene precipitation onset in crude oil and in toluene solutions of asphaltic material were not the same, the stability of both sample A and sample B were in the same order: crude oil > solid residue > asphaltenes. This indicates that the components in both the solid residue and crude oil acted to stabilize the asphaltenes.

Determination of asphaltene precipitation onset of the systems containing different proportions of *n*-heptane/toluene and detection by ultraviolet (UV) spectrometry.

The asphaltene precipitation onset assays using titration with *n*-heptane and monitoring by NIR spectrometry are relatively easy to perform. However, they do not provide information regarding the quantity of asphaltenes precipitated. To determine this quantity, it is possible to use a procedure involving preparation of dispersions with distinct solvents and constant asphaltenes concentration, with monitoring of the concentration of asphaltenes that remains in solution by ultraviolet spectrometry. The procedure requires first obtaining a response curve of

Table 3. Asphaltenes precipitation onset obtained by near-infrared (NIR) spectroscopy

Extraction method	Sample	Concentration / (g L ⁻¹)	Onset / (mL _{<i>n</i>-heptane} g ⁻¹ sample)	Onset / (mL _{<i>n</i>-heptane} mL ⁻¹ sample)
–	PET A	–	3.5	–
–	PET B	–	3.2	–
1	ASPH A	5	–	1.4
	ASPH B	5	–	1.9
	ASPH C	5	–	1.7
2	SR A	15	–	3.0
	SR B	15	–	2.4

PET: crude oil; ASPH: asphaltenes; SR: solid residue.

absorption intensity in function of the concentration of each type of asphaltene studied.

Response curves of absorption intensity in function of concentration

Table 4 presents the linear equations obtained for each of the systems. The error associated with the concentration was obtained based on regression analysis with 95% confidence level. With these curves and knowledge of optical path length (2 mm), it was possible to determine, using Lambert-Beer's law,⁶⁴ the mass absorptivity (ϵ), which quantifies the light absorption capacity of a determined molecule at a determined wavelength.

Figure 4 shows the results of asphaltene concentration in solution in function of the content of *n*-heptane in the mixture with toluene, for the asphaltene system of PET A obtained by method 1 (ASPH A). For low levels of *n*-heptane, the concentration of asphaltenes in solution remained unchanged, indicating that the entire mass of asphaltenes remained in solution. When the *n*-heptane content became sufficient to start the asphaltene precipitation, there was a decline of the concentration of asphaltenes that remained in solution. The reduction of the concentration of asphaltenes

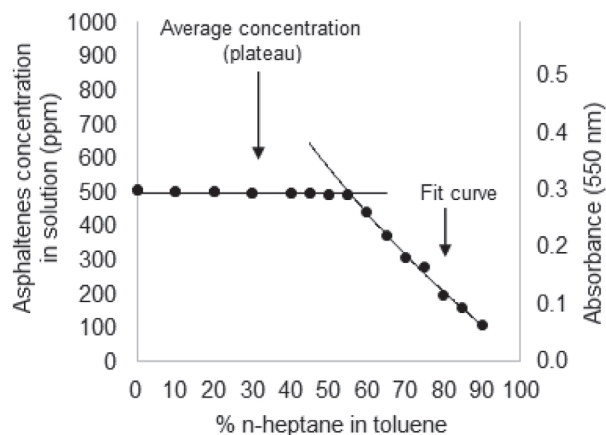


Figure 4. Precipitation test by UV spectroscopy of the asphaltenes extracted from sample PET A by method 1 at concentration of 0.5 g L⁻¹.

Table 4. Determination of the absorptivity

Extraction method	Sample	Wavelength / nm	Curve equation (R ²)	ϵ / (L mg ⁻¹ m ⁻¹)
1	ASPH A	550	$y = (63 \pm 3) \times 10^{-5}x$ (0.996)	0.315
	ASPH B	450	$y = (90 \pm 6) \times 10^{-5}x$ (0.991)	0.450
	ASPH C	500	$y = (69 \pm 3) \times 10^{-5}x$ (0.994)	0.345
2	ASPH from SR A	550	$y = (58 \pm 2) \times 10^{-5}x$ (0.997)	0.290
	SR A	450	$y = (69 \pm 4) \times 10^{-5}x$ (0.992)	0.345
	SR B	400	$y = (68 \pm 6) \times 10^{-5}x$ (0.983)	0.340

R²: coefficient of determination; ϵ : mass absorptivity; ASPH: asphaltenes; SR: solid residue.

dissolved in the medium became more intense as the level of *n*-heptane in the solvent mixture increased, since the greater content of *n*-heptane reduces the asphaltene solubilization power of the mixture of solvents. To estimate the percentage of *n*-heptane necessary to start the asphaltene precipitation, we used three methods: (i) method A, at the intersection of the line corresponding to the average concentration (plateau) with the curve fitted to the points where the concentration decreases with increasing content of *n*-heptane (Figure 4); (ii) method B, at the last point of the asphaltenes concentration before it started to decline; and (iii) method C, by calculating the inflection point of a curve fitted to the experimental data employing the TableCurve 2D software⁶⁵ (see SI section).

Table 5 reports, for all the samples, the estimated *n*-heptane content values in the *n*-heptane/toluene mixture that promoted the asphaltene precipitation onset, utilizing the three mentioned methods. Since these methods produced similar results, we decided to use the value obtained by the most direct method (method B). Besides this, method C presented larger deviations than the other two in the case of the asphaltene A stock solution (most concentrated).

It was necessary to increase the content of *n*-heptane in solution to start the asphaltene precipitation in the case of solid residues A and B (SR A and SR B) more than when only asphaltene C7I was in solution. This agrees with the results obtained previously, that in crude oil other components alter the solubility of asphaltenes, with resins and aromatics being responsible for the solvency conditions of the medium due to the presence of aromatic rings in their composition. Although it was not possible to directly compare the results obtained by the two techniques (except for asphaltenes A), since we used solutions with different stock solution concentrations for the onset ascertained by the UV and NIR spectroscopic methods, the results were close. In other words, in both techniques, although the same precipitation onset was not obtained, the asphaltenes were more stable in the solid residue, since

Table 5. Estimate of the concentration of *n*-heptane in the *n*-heptane/toluene mixture that promoted the onset of asphaltene precipitation

Extraction method	Sample	Asphaltenes concentration / (g L ⁻¹)	Prediction method of the onset / (% <i>n</i> -heptane)			Onset ^a / (mL <i>n</i> -heptane per mL sample)
			A	B	C	
1	ASPH A	0.5	57	55	53	1.2
		1.0	49	50	48	1.0
		5.0	50	50	58	1.0
	ASPH B	0.5	57	55	57	1.2
	ASPH C	0.5	57	55	55	1.2
2	ASPH from SR A	0.5	56	55	52	1.2
	SR A	0.5	71	70	75	2.3
	SR B	0.5	63	60	65	1.5

^aCalculated from the proportion of *n*-heptane/toluene for precipitation onset, utilizing method B; ASPH: asphaltenes, SR: solid residue; A: at the intersection of the line corresponding to the average concentration with the curve fitted to the points where the concentration decreases with increasing content of *n*-heptane; B: at the last point of the asphaltenes concentration before it started to decline; C: by calculating the inflection point of a curve fitted to the experimental data.

the precipitation onset was higher for the solid residue than for the asphaltenes. NIR spectroscopy can measure more variations in *n*-heptane/toluene proportions, within the same range, than UV spectroscopy, making the onset determination more accurate. In turn, UV spectroscopy establishes the balance between the liquid and solid phases due to the resting time (2 h) and, although this affects the kinetic of the process,^{66,67} it is able to determine the quantity of asphaltenes precipitated, unlike the NIR counterpart, which is more dynamic and hence more suitable from the operational standpoint.

The influence of concentration of the asphaltic material on the asphaltene precipitation onset also was assessed by the UV technique. This analysis was carried out with the asphaltene C7I extracted from PET A by method 1 (ASPH A), employing asphaltene concentrations in the stock solutions of 0.5, 1.0 and 5.0 g L⁻¹. To better compare the results, we converted the values of asphaltene concentration in solution to fractional values of precipitated asphaltenes, which were plotted in function of *n*-heptane content in the mixture with toluene (Figure 5). A 10-fold increase in the asphaltene concentration in the medium (from 0.5 to 5.0 g L⁻¹) led to a decrease of 5% in the precipitation onset, which can be considered to have little relevance.

Above the precipitation onset, the fraction of precipitated asphaltenes increased as the concentration of the stock solution rose. In the system with 90% *n*-heptane, the precipitated fractions were 0.78, 0.89 and 0.96 for the stock solutions of asphaltenes at 0.5, 1.0 and 5.0 g L⁻¹, respectively. This behavior can be interpreted as follows: with higher concentration, there are more asphaltene molecules in solution, and to attain the same equilibrium between the solid and liquid phases, a larger quantity of asphaltenes have to precipitate. This fact can

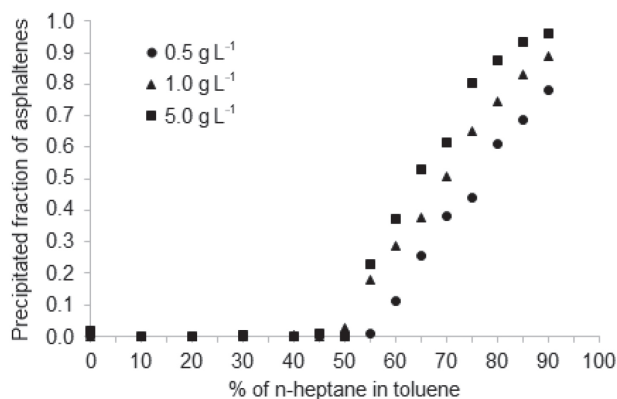


Figure 5. Fraction precipitated of asphaltene C7I (extracted from PET A by method 1) in function of the content of *n*-heptane for systems containing different initial concentrations of dissolved asphaltenes.

also be explained based on the asphaltene aggregation process, whereby the aggregation degree rises along with the asphaltene concentration in solution.⁶⁸ The fractions precipitated for the different systems studied, all at asphaltene concentration of 0.5 g L⁻¹ in the stock solution and 90% *n*-heptane, were: ASPH A = 0.78; ASPH B = 0.70; ASPH C = 0.70; ASPH from SR A = 0.75; SR A = 0.53; and SR B = 0.65. As can be noted from comparing these values, the precipitated fractions were concordant among the asphaltenes. However, although solid residue A had a higher asphaltene fraction than solid residue B (Table 2), about 12% more asphaltenes precipitated from SR B than SR A. This confirms what was mentioned previously, that the greater content of aromatics from SR A in comparison with SR B, although it contains a smaller content of resins, was responsible for stabilizing the asphaltenes.

From the precipitation assays, we obtained the asphaltenes solubility in the solvent mixtures, which allowed to determine their solubility parameters.

Estimate of the solubility parameter of the asphaltic material

The solubility parameter of the asphaltic material was estimated based on the Scatchard-Hildebrand equation (equation 3), the combination of Scatchard-Hildebrand equation and Flory-Huggins theory (equation 5), an empirical correlation (equation 7), and the results of the precipitation assays. The working temperature was $T = 25\text{ }^{\circ}\text{C}$ or 298.15 K (room temperature).

Solubility parameter of the solvent

Based on the solubility parameter table values for toluene ($18.2\text{ MPa}^{0.5}$)^{36,38} and *n*-heptane ($15.3\text{ MPa}^{0.5}$)^{36,40} we calculated the Hildebrand solubility parameter of the solvents (mixtures of *n*-heptane and toluene) using the weighted average of the volumetric fractions, obtaining values of 18.2, 17.9, 17.6, 17.3, 17.0, 16.8, 16.5, 16.2, 15.9, 15.6 and $15.3\text{ MPa}^{0.5}$, respectively, for the *n*-heptane levels of 0, 10, 20, 30, 40, 50, 60, 70, 80, 90 and 100%. A variation of 10 percentage points in the content of *n*-heptane in the mixture (e.g., from 50 to 60%) diminished the mixture's solubility parameter by about $0.3\text{ MPa}^{0.5}$. Hence, it can be assumed that the decrease of 5% in the precipitation onset with a 10-fold increase in the concentration of asphaltenes in the stock solution was not very relevant for the objectives of this study. Therefore, we did not consider a possible effect of this concentration.

Density and molar mass

The densities of the asphaltenes and the solid residues were estimated based on equation 8.²⁰

$$\frac{1}{\rho_{\text{mixt}}} = \frac{1}{\rho_{\text{T}}} + \left(\frac{1}{\rho_{\text{i}}} - \frac{1}{\rho_{\text{T}}} \right) x_{\text{i}} \quad (8)$$

where ρ_{mixt} , ρ_{T} , ρ_{i} are the density (kg m^{-3}) of the mixture, toluene and solute *i* (asphaltenes or solid residue),

respectively; and x_{i} is the mass fraction of solute *i*. We then plotted graphs of $1/\rho_{\text{mixt}}$ versus $x_{\text{asphaltenes}}$ for each of the systems, and calculated the densities (Table 6) according to the equations of the lines and applying equation 9.

$$D = \frac{1}{\rho_{\text{i}}} - \frac{1}{\rho_{\text{T}}} \leftrightarrow \rho_{\text{i}} = \frac{1}{D + \frac{1}{\rho_{\text{T}}}} = \frac{1}{D + O} \quad (9)$$

where *D* and *O* are the angular coefficient and the linear coefficient of the line, respectively. The errors associated with the angular and linear coefficients were obtained by regression analysis, with a confidence level of 95%. By applying the density values, we determined the molar masses of the fractions studied using equation 10.⁶⁹ The results are reported in Table 6.

$$\rho_{\text{i}} = 670\text{MM}_{\text{i}}^{0.0639} \leftrightarrow \text{MM}_{\text{i}} = \sqrt[0.0639]{\frac{\rho_{\text{i}}}{670}} \quad (10)$$

where ρ_{i} is the density (kg m^{-3}) of solute *i* and MM_{i} is the molar mass (g mol^{-1}) of solute *i*.

In relation to density, the values obtained for the pure asphaltenes were very near that suggested in the literature ($1,200\text{ kg m}^{-3}$).^{16,61} Luo and Gu⁷⁰ obtained a value of $1,175\text{ kg m}^{-3}$ for asphaltenes from a heavy crude sample based on the content of asphaltenes (% m m^{-1} of the sample), the density of the oil itself and the density of the deasphalted oil. Thus, the method employed in this work can be used to estimate the density of these fractions of crude oil simply and rapidly, without the need for sophisticated equipment. It is important to note that the fact the densities of the ASPH B and SR B were very near can indicate inefficiency of the process of purifying these asphaltenes.⁷¹ The estimated molar mass values were higher than those obtained experimentally by the vapor pressure osmometry (VPO) technique (750 g mol^{-1} ,²⁴ 850 g mol^{-1} ,⁷² $2,000\text{ g mol}^{-1}$)¹⁹ and by mass spectrometry²⁵ (MALDI-TOF). Both the density and molar mass of the asphaltenes were higher than the values obtained for the

Table 6. Density and molar mass calculated for the asphaltenes and solid residues

Extraction method	Sample	Adjustment line equation (R ²)	Density / (kg m^{-3})	MM / (g mol^{-1})
1	ASPH A	$y = (-28 \pm 4) \times 10^{-2}x + (11538 \pm 3) \times 10^{-4}$ (0.997)	1142	4184
	ASPH B	$y = (-24 \pm 3) \times 10^{-2}x + (11538 \pm 2) \times 10^{-4}$ (0.999)	1091	2059
	ASPH C	$y = (-29 \pm 6) \times 10^{-2}x + (11538 \pm 4) \times 10^{-4}$ (0.995)	1159	5316
2	ASPH from SR A	$y = (-29 \pm 1) \times 10^{-2}x + (11538 \pm 1) \times 10^{-4}$ (1.000)	1153	4918
	SR A	$y = (-22 \pm 3) \times 10^{-2}x + (11538 \pm 4) \times 10^{-4}$ (0.998)	1074	1608
	SR B	$y = (-20 \pm 2) \times 10^{-2}x + (11539 \pm 2) \times 10^{-4}$ (0.999)	1053	1176

R²: coefficient of determination; MM: molar mass; ASPH: asphaltenes; SR: solid residue.

respective solid residues. This result makes sense, because the solid residues are composed by combinations of molecules with high molar mass (asphaltenes) with molecules having lower molar mass, while the asphaltenes are composed only of molecules with high molar mass.

Molar fraction and volumetric fraction of the solute

The solubility metric of the Scatchard-Hildebrand equation is expressed in terms of the molar fractions of asphaltenes. These fractions can be obtained from the mass fraction results of asphaltenes that precipitate, established by precipitation tests. The number of moles (n) of each solvent s (toluene or n -heptane) were calculated by equation 11:

$$n_s = \frac{V_s \rho_s}{MM_s} \quad (11)$$

where ρ_s , MM_s and V_s are the density (kg m^{-3}), molar mass (kg mol^{-1}) and volume (m^3) of solvent s , respectively. For this purpose, we measured the densities of toluene and n -heptane with a density meter and obtained respective values of 866.68 and 683.87 kg m^{-3} , which are in accordance with the literature.^{73,74} For molar mass, we used values of 92.14 and 100.21 g mol^{-1} , respectively, for toluene and n -heptane. By introducing in the system 1 mL of a solution of asphaltic material in toluene (with known concentration), it was possible to calculate the initial number of moles of the asphaltenes in solution. The final molar fraction of asphaltenes in solution was obtained by dividing the number of moles of the asphaltenes present at the end of the test (knowing the initial number of moles and the fraction of asphaltenes that precipitated in each test) by the total number of moles of the solution.

In the case of the equation based on the Flory-Huggins theory (equation 5), the solubility is expressed as a volumetric fraction of the solute, which was calculated with equation 12. Besides this, we considered the excess molar volume of the n -heptane/toluene mixtures, where the real molar volume of the mixture is equal to the sum of the ideal molar volume (equation 13) with the excess molar volume (equation 14, in $\text{cm}^3 \text{mol}^{-1}$).⁷⁵

$$\phi_i = \frac{n_{i,\text{final}} MM_i}{V_{\text{mixt}}} \quad (12)$$

$$V_{\text{mixt}}^I = x_H v_H + x_T v_T \quad (13)$$

$$V_{\text{mixt}}^E = x_H x_T \left[0.5720 + 0.0058(x_H - x_T) + 0.0641(x_H - x_T)^2 \right] \quad (14)$$

where ϕ_i and n_i are the volumetric fraction and number of moles of solute i , respectively; and v_H , v_T , x_H and x_T are the molar volumes and molar fractions of n -heptane and toluene, respectively.

By introducing in the respective equations all the previously estimated/calculated parameters, we obtained the results presented in Table 7. The solubility parameter range is related to the results obtained just from the precipitation onset condition (since it is only possible to make the simplifications inherent to the theories used to estimate the solubility parameters from this condition) to heptane/toluene 90/10 condition. This range can be explained by the fact that asphaltenes are a fraction composed by molecules with diverse solubilities. Hence, as the fraction of n -heptane increases, an asphaltene fraction with lower solubility parameter precipitates, since the solubility parameter of the mixture declines. We also compared the solubility parameters obtained previously

Table 7. Estimate of the solubility parameters (δ) of the asphaltenes based on the Scatchard-Hildebrand (SH) equation, the combination of SH equation and Flory-Huggins (FH) theory, and an empirical correlation,⁶⁹ and estimate of the constant K suggested by Yarranton and Masliyah²⁰ for the samples under study

Extraction method	Sample	Sample concentration / (g L^{-1})	δ / $\text{MPa}^{0.5}$			
			Empirical correlation	SH equation	SH equation / FH theory	K / (J g^{-1})
1	ASPH A	0.5		19.6-18.8	21.7-20.6	336-306
	ASPH A	1.0	20.5	19.8-18.8	21.8-20.6	340-306
	ASPH A	5.0		19.5-18.7	21.7-20.6	333-309
	ASPH B	0.5	20.0	20.7-19.8	22.2-21.2	375-343
	ASPH C	0.5	20.6	19.3-18.4	21.6-20.4	326-296
2	ASPH from SR A	0.5	20.6	19.4-18.5	21.6-20.4	330-300
	SR A	0.5	19.9	20.8-20.3	22.0-21.4	379-361
	SR B	0.5	19.7	21.8-21.1	22.9-22.0	416-390

ASPH: asphaltenes; SR: solid residue.

with the values obtained by the empirical correlation,²⁰ assuming a value of $K = 367 \text{ J g}^{-1}$.⁷⁶ This constant was obtained from the correlation, with adjustment of its value until obtaining good concordance between the experimental solubility values and those calculated by the model at 23 °C. The results of this estimate are also presented in Table 7. The values obtained for the solubility parameters of the asphaltenes are within the range of values reported in the literature (between 19 and 23 MPa^{0.5}).^{77,78}

The variation of the solubility parameters obtained by the Scatchard-Hildebrand equation and the Flory-Huggins theory can be attributed to the fact the latter considers a correction factor due to the variation of entropy of the system. This correction is associated with variation of the molar volume of the mixture, which in turn is obtained based on the molar masses and respective densities of the solvents. Since the molar mass of the asphaltic material is typically one order of magnitude greater than that of the solvent, and was estimated based on a correlation, it would be interesting to measure them experimentally through techniques normally employed for this purpose, to confirm the validity of such correlation for the samples used. By considering the entropy (Flory-Huggins theory), the solubility parameter increases about 1 to 2 unities. The empiric correlation to determine solubility parameter, which does not consider entropic contribution, present values closer to those obtained by Scatchard-Hildebrand (SH) equation.

For asphaltenes extracted from petroleum A (ASPH A), it was observed that, although this concentration only slightly influenced the asphaltene precipitation onset (5% when increasing the concentration 10-fold), this does not produce significant variations in the estimated solubility parameter of the asphaltenes in the concentration interval studied (0.5 to 5.0 g L⁻¹). We also compared the results obtained for the ASPH A (asphaltene extracted from petroleum A using *n*-heptane) and ASPH from SR A (asphaltene extracted from solid residue A using *n*-heptane), and we observed close similarity, both in the precipitation onset and the solubility parameters. Further regarding the results presented in Table 7, we obtained a different solubility parameter for each asphaltic material.

The solubility parameters obtained in this study, based on the theories described, for the solid residues (SR A and SR B), are higher than the solubility parameters of the asphaltenes extracted from the respective crude oil samples by method 1 (ASPH A and ASPH B). Under the fractionation conditions used in method 2 (high pressure and temperature), the flocculant present solubility parameter around 13 MPa^{0.5},⁷⁹ resulting in a larger amount of molecules extracted than by method 1 (δ of *n*-heptane = 15.3 MPa^{0.5}).³⁶

Therefore, in the solid residue, the amount of aggregates increases and, most likely, more compact and lower molar volume structures are formed. The presence of resins can also contribute to the lower size of the aggregates. Such behavior leads to an increase in the calculated solubility parameter of the solid residue when compared with asphaltenes extracted by method 1.

The fact of not having obtained the value of the constant K based on fitting the data for each asphaltic material, as suggested by other authors,²⁰ can explain the difference in the solubility parameters obtained by the two methods. However, even in these situations, we believe this correlation is a simple way to estimate these parameters for asphaltenes, since the results found in this work are near those obtained by the Scatchard-Hildebrand (SH) equation. Therefore, we estimated the value of the constant K to obtain the upper and lower limits of the solubility parameters by the Scatchard-Hildebrand equation. All the values obtained for the constant K were within, or very close to, the interval suggested by Yarranton and Masliyah²⁰ (270-398 J g⁻¹), and could be the most suitable values for the respective samples. However, this should be confirmed by fitting experimental data. Yarranton and co-workers⁸⁰ concluded that an increase of the constant K is intrinsically related to the decline of solubility.

These observations can be summarized as follows: (i) the quantity of asphaltenes that precipitates increases with rising concentration of asphaltenes in solution, but the solubility parameter of the asphaltenes that precipitated remain the same for a given solvent medium with a given solubility parameter; and (ii) the solubility parameter of the precipitated asphaltene molecules increases with rising solubility parameter of the solvent medium, and in a narrow range including the value of 19 MPa^{0.5}, no precipitation occurs.

Conclusions

Through analysis of the behavior of asphaltenes in a simplified model (*n*-heptane/toluene mixtures), we found that the solubility parameter of asphaltene fraction C7I, obtained from two heavy crude oil samples (°API < 22.3) and an asphaltic residue (estimated by the Scatchard-Hildebrand equation, Flory-Huggins theory and empirical correlation) was within the range of values reported in the literature (between 19 and 23 MPa^{0.5}).^{77,78}

The asphaltene precipitation onset reduced by about 5% when the concentration of asphaltene C7I increased from 0.5 to 5.0 g L⁻¹. Despite the expectation that as the concentration of asphaltenes increased, their propensity to precipitate would also rise,⁶⁸ at the concentrations studied

here this correlation did not occur linearly. When inducing asphaltene precipitation of more concentrated solutions, the quantity of material precipitated was greater. We believe this occurred because as the concentration rises, there are more asphaltene molecules in solution, and to attain the same balance between the solid and liquid phases, it is necessary for a larger quantity of asphaltenes to precipitate. Indeed, the quantity of asphaltenes that precipitates increases with rising concentration of asphaltenes in solution, but the solubility parameter of the asphaltenes that precipitated remain the same for a given solvent medium with a given solubility parameter.

The asphaltenes isolated by the two extraction methods presented similar values, both for precipitation onset and solubility parameter. Despite the differences of the extraction methods regarding the conditions of temperature, pressure and solvent used, it is possible that the purification step (using *n*-heptane) of the solid residue obtained by method 2 led to obtaining asphaltene fraction C7I very similar to the asphaltenes obtained by method 1 (also using *n*-heptane), since they came from the same crude oil sample.

The use of different methodologies slightly affect the asphaltenes precipitation onset: for asphaltenes extracted from crude oil A at 5 g L⁻¹ in toluene, the onset values were 1.4 mL of *n*-heptane *per* g of sample and 1.0 mL of *n*-heptane *per* g of sample when using, respectively, near-infrared (NIR) and ultraviolet-visible (UV) spectroscopic techniques. The lower value obtained by UV is in agreement with the resting procedure used, which enable the formation of aggregates in advance due to the kinetic of the aggregation process.^{45,46}

Knowledge of the exact conditions of the occurrence of asphaltene precipitation in real systems (crude oil in the conditions found in nature, at refineries or during transport) is important to avoid the problems associated with deposition of this fraction, to minimize costs. The system studied in this work (solution of asphaltenes in toluene), although very simple, allowed minimizing the variables of more complex systems used to learn the parameters of asphaltenes, enabling studying the influence of other fractions (saturates, aromatics and resins) on the stabilization of asphaltenes. For the samples investigated in this work, the aromatic fraction had stronger action in stabilizing the asphaltenes than the other fractions in the crude oil samples.

Supplementary Information

Supplementary data (FTIR results of crude oil and its fractions, and equations to fit the experimental data from

the UV tests using three different methods to identify the asphaltenes precipitation onset) are available free of charge at <http://jbcs.sbq.org.br> as PDF file.

Acknowledgments

We thank CNPq (307193/2016-0), CAPES, FAPERJ (E-26/202.822/2017), ANP and Petrobras for financial support.

Author Contributions

Faissen B. Lordeiro was responsible for conceptualization, data curation, formal analysis, investigation, writing original draft; Rodrigo Altoé for investigation; Daniela Hartmann for formal analysis, investigation, writing-review and editing; Eduardo J. M. Filipe for supervision, writing-review and editing; Gaspar González for conceptualization, supervision; Elizabete F. Lucas for writing original draft, writing-review and editing, visualization, project administration, resources, funding acquisition.

References

1. Speight, J. G.; Özüim, B.; *Petroleum Refining Processes*; Marcel Dekker: New York, 2002.
2. Wauquier, J.-P.; *Petroleum Refining: Crude Oil Petroleum Products, Process Flowsheets*, vol. 1; Éditions Technip: Paris, 1995.
3. Werner, A.; Behar, F.; de Hemptinne, J. C.; Behar, E.; *Fluid Phase Equilib.* **1998**, *147*, 343.
4. Sharma, M. K.; Yen, T. F.; *Asphaltene Particles in Fossil Fuel Exploration, Recovery, Refining, and Production Processes*; Springer: New York, 1994.
5. Speight, J. G.; *Oil Gas Sci. Technol.* **2004**, *59*, 467.
6. Chen, C.; Guo, J.; An, N.; Pan, Y.; Li, Y.; Jiang, Q.; *Pet. Sci.* **2012**, *9*, 551.
7. Chen, C.; Guo, J.; An, N.; Ren, B.; Li, Y.; Jiang, Q.; *Pet. Sci.* **2013**, *10*, 134.
8. Dong, Z.-X.; Wang, J.; Liu, G.; Lin, M.-Q.; Li, M.-Y.; *Pet. Sci.* **2014**, *11*, 174.
9. Honse, S. O.; Mansur, C. R. E.; Lucas, E. F.; *J. Braz. Chem. Soc.* **2012**, *23*, 2204.
10. Kilpatrick, P. K.; *Energy Fuels* **2012**, *26*, 4017.
11. Qiao, P.; Harbottle, D.; Tchoukov, P.; Masliyah, J.; Sjoblom, J.; Liu, Q.; Xu, Z.; *Energy Fuels* **2017**, *31*, 3330.
12. Shahsavani, B.; Malayeri, M. R.; Riazi, M.; *J. Mol. Liq.* **2019**, *295*, 111688.
13. D'Avila, F. G.; Silva, C. M. F.; Steckel, L.; Ramos, A. C. S.; Lucas, E. F.; *Energy Fuels* **2020**, *34*, 4095.

14. Ismail, I.; Kazemzadeh, Y.; Sharifi, M.; Riazi, M.; Malayeri, M. R.; Cortés, F.; *J. Mol. Liq.* **2020**, *299*, 112125.
15. Mullins, O. C.; Sheu, E. Y.; *Structures and Dynamics of Asphaltenes*; Springer: New York, 1998.
16. Akbarzadeh, K.; Hammami, A.; Kharrat, A.; Zhang, D.; Allenson, S. J.; Creek, J.; Kabir, S.; Jamaluddin, A. K. M.; Marshall, A. G.; Rodgers, R. P.; Mullins, O. C.; Solbakken, T.; *Oilfield Rev.* **2007**, *19*, 22.
17. Lucas, E. F.; Ferreira, L. S.; Khalil, C. N. In *Encyclopedia of Polymer Science and Technology*; Mark, H. F., ed.; John Wiley & Sons: New Jersey, 2015.
18. Hartmann, D.; Lopes, H. E.; Teixeira, C. L. S.; Oliveira, M. C. K.; Gonzalez, G.; Lucas, E. F.; Spinelli, L. S.; *Energy Fuels* **2016**, *30*, 3693.
19. Boduszynski, M. M.; *Energy Fuels* **1987**, *1*, 2.
20. Yarranton, H. W.; Masliyah, J. H.; *AIChE J.* **1996**, *42*, 3533.
21. Martín-Martínez, F. J.; Fini, E. H.; Buehler, M. J.; *RSC Adv.* **2015**, *5*, 753.
22. Barrera, D. M.; Ortiz, D. P.; Yarranton, H. W.; *Energy Fuels* **2013**, *27*, 2474.
23. Dickie, J. P.; Yen, T. F.; *Anal. Chem.* **1967**, *39*, 1847.
24. McKenna, A. M.; Marshall, A. G.; Rodgers, R. P.; *Energy Fuels* **2013**, *27*, 1257.
25. Ferreira, S. R.; Barreira, F. R.; Spinelli, L.; Seidl, P.; Leal, K. Z.; Lucas, E. F.; *Quim. Nova* **2016**, *39*, 26.
26. Mullins, O.; *The Molecular Weight and Molecular Structure of Asphaltenes*, available at <https://sites.ualberta.ca/dept/chemeng/asphaltenes/Mullins.htm>, accessed in November 2020.
27. Lee, J. M.; Shin, S.; Ahn, S.; Chun, J. H.; Lee, K. B.; Mun, S.; Jeon, S. G.; Na, J. G.; Nho, N. S.; *Fuel Process. Technol.* **2014**, *119*, 204.
28. Silva, H. S.; Alfara, A.; Vallverdu, G.; Bégué, D.; Bouyssié, B.; Baraille, I.; *Pet. Sci.* **2019**, *16*, 669.
29. Camargo, R. A.; Ramos, A. C. S.; Gatto, D. A.; Beltrame, R.; Monks, J. L. F.; *Braz. J. Pet. Gas* **2019**, *13*, 265.
30. Alimohammadi, S.; Zendejboudi, S.; James, L.; *Fuel* **2019**, *252*, 753.
31. Rashid, Z.; Wilfred, C. D.; Gnanasundaram, N.; Arunagiri, A.; Murugesan, T.; *J. Pet. Sci. Eng.* **2019**, *176*, 249.
32. Balestrin, L. B. S.; Loh, W.; *J. Braz. Chem. Soc.* **2020**, *31*, 230.
33. Shoukry, A. E.; El-Banbi, A. H.; Sayyoub, H.; *Pet. Sci.* **2020**, *17*, 232.
34. Celia-Silva, L. G.; Vilela, P. B.; Morgado, P.; Lucas, E. F.; Martins, L. F. G.; Filipe, E. J. M.; *Energy Fuels* **2020**, *34*, 1581.
35. Barton, A. F. M.; *Chem. Rev.* **1975**, *75*, 731.
36. Barton, A. F. M.; *Handbook of Solubility Parameters and Other Cohesion Parameters*, 2nd ed.; CRC Press: Boca Raton, 1991.
37. Acevedo, S.; Castro, A.; Vasquez, E.; Marcano, F.; Ranaudo, M. A.; *Energy Fuels* **2010**, *24*, 5921.
38. Sato, T.; Araki, S.; Morimoto, M.; Tanaka, R.; Yamamoto, H.; *Energy Fuels* **2014**, *28*, 891.
39. Redelius, P.; *Energy Fuels* **2004**, *18*, 1087.
40. Hansen, C. M.; *Hansen Solubility Parameters: A User's Handbook*; CRC Press: Boca Raton, 2007.
41. Carvalho, S. P.; Lucas, E. F.; Gonzalez, G.; Spinelli, L. S.; *J. Braz. Chem. Soc.* **2013**, *24*, 1998.
42. Subramanian, S.; Simon, S.; Sjöblom, J.; *J. Disp. Sci. Technol.* **2016**, *37*, 1027.
43. Jones, C. H.; *Marine Fuels: A Symposium*, 878th ed.; ASTM International: Philadelphia, 1985, p. 228.
44. Hirschberg, A.; deJong, L. N. J.; Schipper, B. A.; Meijer, J. G.; *Soc. Pet. Eng. J.* **1984**, *24*, SPE-11202-PA.
45. Maqbool, T.; Balgoa, A. T.; Fogler, H. S.; *Energy Fuels* **2009**, *23*, 3681.
46. Duran, J. A.; Schoeggel, F. F.; Yarranton, H. W.; Vilas Bôas Fávero, C.; Fogler, H. S.; *Energy Fuels* **2020**, *34*, 1408.
47. Marcano, F.; Moura, L. G. M.; Cardoso, F. M. R.; Rosa, P. T. V.; *Energy Fuels* **2015**, *29*, 2813.
48. Soleymanzadeh, A.; Yousefi, M.; Kord, S.; Mohammadzadeh, O.; *J. Pet. Explor. Prod. Technol.* **2019**, *9*, 1375.
49. IP 143/01: *Standard Methods for Analysis and Testing of Petroleum and Related Products*; Institute of Petroleum of London: London, 2001, available at <https://publishing.energyinst.org/topics/fuel-quality-and-control/ip-test-methods/ip-143-determination-of-asphaltenes-heptane-insolubles-in-crude-petroleum-and-petroleum-products2>, accessed in November 2020.
50. González, G.; Middea, A.; *Colloids Surf.* **1991**, *52*, 207.
51. Silva, J. C.; Maravilha, T. S. L.; Nunes, R. C. P.; Lucas, E. F.; *J. Mater. Educ.* **2019**, *41*, 149.
52. Altoé, R.; Oliveira, M. C. K.; Lopes, H. E.; Teixeira, C.; Cirilo, L. C. M.; Lucas, E. F.; Gonzalez, G.; *Colloids Surf., A* **2014**, *445*, 59.
53. Garreto, M. S. E.; Gonzalez, G.; Ramos, A. C. S.; Lucas, E. F.; *Chem. Chem. Technol.* **2010**, *4*, 317.
54. Garreto, M. S. E.; Mansur, C. R. E.; Lucas, E. F.; *Fuel* **2013**, *113*, 318.
55. <http://www.petroleum.co.uk/sweet-vs-sour>, accessed in November 2020.
56. Ashtari, M.; Bayat, M.; Sattarin, M.; *Energy Fuels* **2011**, *25*, 300.
57. González, G.; Sousa, M. A.; Lucas, E. F.; *Energy Fuels* **2006**, *20*, 2544.
58. Barreira, F. R.; Reis, L. G.; Reis, W. R. D.; Nunes, R. C. P.; Filipakis, S. D.; Lucas, E. F.; *Energy Fuels* **2018**, *32*, 10391.
59. Nunes, R. C. P.; Valle, M. R. T.; Reis, W. R. D.; Aversa, T. M.; Filipakis, S. D.; Lucas, E. F.; *J. Braz. Chem. Soc.* **2019**, *30*, 1241.
60. Figueira, J. N.; Simão, R. A.; Soares, B. G.; Lucas, E. F.; *Rev. Fuentes, Reventon Energ.* **2017**, *15*, 7.
61. Sheu, E. Y.; Mullins, O. C.; *Asphaltenes: Fundamentals and Applications*; Springer: New York, 1995.

62. Spiecker, P. M.; Gawrys, K. L.; Trail, C. B.; Kilpatrick, P. K.; *Colloids Surf., A* **2003**, 220, 9.
63. Carbognani, L.; Espidel, J. Y.; *Vision Tecnol.* **1995**, 3, 35.
64. Perkampus, H.-H.; *UV-VIS Spectroscopy and Its Applications*; Springer-Verlag: Berlin, 1992.
65. *TableCurve 2D Software*, v.5.01; Systat Software, San Jose, United States, 2004, available at <http://www.systat.com/>, accessed in November 2020.
66. Fávero, C. V. B.; Maqbool, T.; Hoepfner, M.; Haji-Akbari, N.; Fogler, H. S.; *Adv. Colloid Interface Sci.* **2017**, 244, 267.
67. Balestrin, L. B. S.; Francisco, R. D.; Bertran, C. A.; Cardoso, M. B.; Loh, W.; *Energy Fuels* **2019**, 33, 4748.
68. Painter, P.; Veytsman, B.; Youtcheff, J.; *Energy Fuels* **2014**, 28, 2472.
69. Akbarzadeh, K.; Dhillon, A.; Svrcek, W. Y.; Yarranton, H. W.; *Energy Fuels* **2004**, 18, 1434.
70. Luo, P.; Gu, Y.; *Fuel* **2007**, 86, 1069.
71. Ancheyta, J.; Trejo, F.; Rana, M. S.; *Asphaltenes: Chemical Transformation during Hydroprocessing of Heavy Oils*; CRC Press: Boca Raton, 2009.
72. Yarranton, H. W.; Ortiz, D. P.; Barrera, D. M.; Baydak, E. N.; Barré, L.; Frot, D.; Eyssautier, J.; Zeng, H.; Xu, Z.; Dechaine, G.; Becerra, M.; Shaw, J. M.; McKenna, A. M.; Mapolelo, M. M.; Bohne, C.; Yang, Z.; Oake, J.; *Energy Fuels* **2013**, 27, 5083.
73. Smallwood, I. M.; *Handbook of Organic Solvent Properties*; Butterworth-Heinemann: London, 1996.
74. Wilson, I. D.; Poole, C. F.; *Handbook of Methods and Instrumentation in Separation Science*, vol. 1; Academic Press: London, 2009.
75. Bravo, R.; Pintos, M.; Amigo, A.; *J. Chem. Thermodyn.* **1991**, 23, 905.
76. Alboudwarej, H.; Akbarzadeh, K.; Beck, J.; Svrcek, W. Y.; Yarranton, H. W.; *AIChE J.* **2003**, 49, 2948.
77. Barton, A. F. M.; *Handbook of Polymer-Liquid Interaction Parameters and Solubility Parameters*; CRC Press: Boca Raton, 1990.
78. Aguiar, J. I. S.; Garreto, M. S. E.; González, G.; Lucas, E. F.; Mansur, C. R. E.; *Energy Fuels* **2014**, 28, 409.
79. de Oliveira, M. C. K.; Lopes, H. E.; Teixeira, C. L.; Chinelatto Jr., L. S.; Gonzalez, G.; Altoé, R.; *Energy Fuels* **2017**, 31, 13198.
80. Akbarzadeh, K.; Alboudwarej, H.; Svrcek, W. Y.; Yarranton, H. W.; *Fluid Phase Equilib.* **2005**, 232, 159.

Submitted: August 3, 2020

Published online: November 13, 2020

